Neutron Capture and Total Cross Section Measurements of Cadmium at the RPI LINAC

Dr. Gregory Leinweber
Bechtel Marine Propulsion Corporation
Gaerttner LINAC Center, Rensselaer Polytechnic Institute

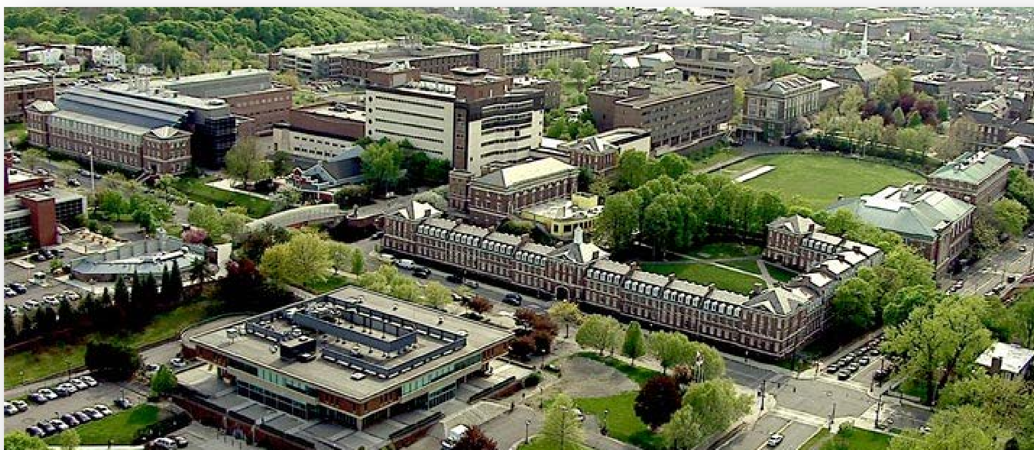

13th International Topical Meeting on Nuclear Applications of Accelerators
31 July-4 August 2017, Quebec, Canada

NNL/RPI Nuclear Data Group

BMPC/NNL
Dr. Greg Leinweber
Dr. Robert C. Block
Dr. Devin Barry
Dr. Michael Rapp
Dr. Kyle Remley
Dr. John Burke
Dr. Tim Trumbull
Brian Epping
Dr. Adam Daskalakis
Dr. Brian McDermott

RPI Faculty
Prof. Yaron Danon - LINAC Director
Prof. Li Liu

Technical Staff
Dr. Ezekiel Blain
Peter Brand
Michael A. Bretti
Matt Gray
Azeddine Kerdoun
Larry Krusieski

Graduate Students
Adam Weltz
Nicholas Thompson
Kemal Ramic
Carl Wendorff
Amanda Youmans
Jesse Brown
Kumar Mohindroo
Amanda Lewis

Undergraduate student
Adam Ney

RPI LINAC History

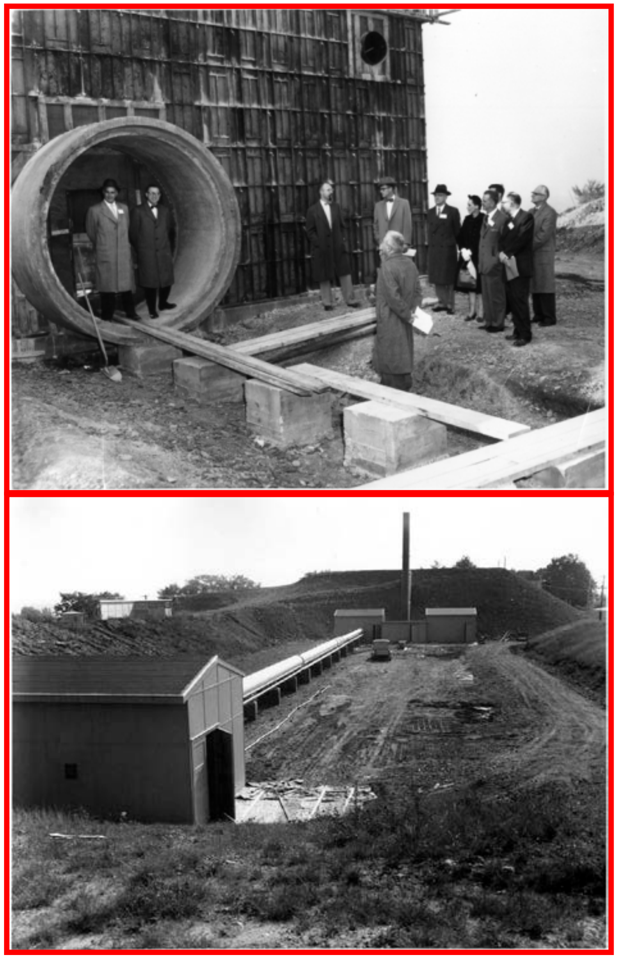

- The RPI LINAC started operation in December 1961
- Working “continuously” ever since
- September 1997- LINAC was designated as Nuclear Historic Landmark by the American Nuclear Society
- Graduated over 170 students who utilized the LINAC as part of their graduate thesis research
- Many years of accumulated experience

RPI LINAC Specifications 2017

	Three Sections (Low Energy Port)	Nine Sections (High Energy Port)
Electron Energy	5 to 25 MeV	25 to over 60 MeV
Pulse Width	6 to 5000 ns	6 to 5000 ns
Peak Current	3A (short pulse: 6 to 50 ns) 400 mA (long pulse: 50 to 5000 ns)	3A (short pulse: 6 to 50 ns) 400 mA (long pulse: 50 to 5000 ns)
Average Power	10 kw@ 17 MeV, 5000 ns	>10 kw@ 60 MeV, 5000 ns
Peak Dose Rate	>10^{11} Rads/sec (in Silicon)	n/a
Neutron Production	n/a	**~4 X 10^{13} neutrons/sec**
Pulse Repetition Rate	Single pulse to 500 pps (short pulse) Single pulse to 300 pps (long pulse)	Single pulse to 500 pps (short pulse) Single pulse to 300 pps (long pulse)

RPI LINAC 2020 - Infrastructure Upgrades

- Constructed a new teaching/research laboratory
- Upgrade the klystrons, modulators, and accelerator sections

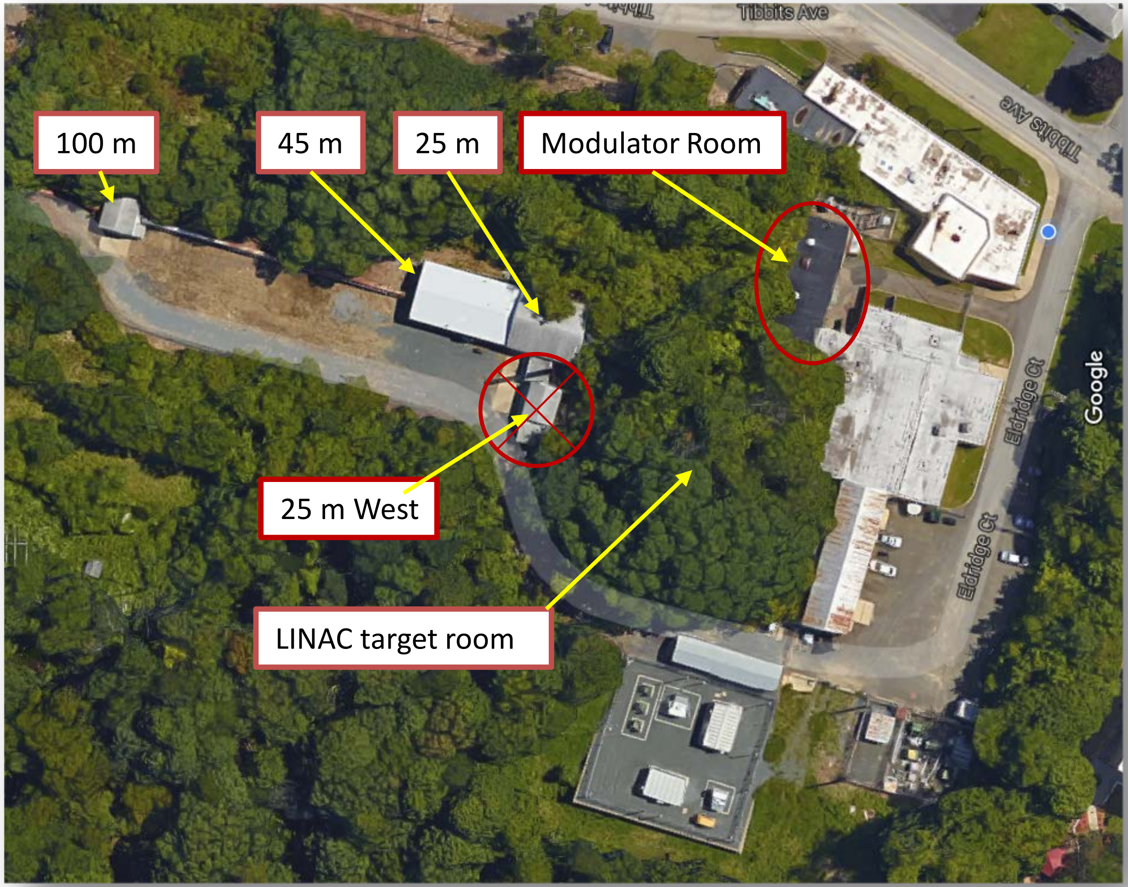

NNL/NCSP/RPI LINAC 2020 Refurbishment and Upgrade Plan

- **Project aims at refurbishment and upgrade of the accelerator**
  - Increase neutron production for short pulses
    - Increase the electron beam energy
    - Modernize the electron beam control system
  - Provide longevity
    - Replace all major components and acquire spares

- **Funded by DOE-NR and NCSP through BMPC/NNL**

RPI LINAC Specifications 2020 Refurbishment

Operation Mode	Pulse Width (ns)	Repetition Rate (Hz)	Beam Energy (MeV)	Pulse Current (μA)	Average Beam Power (kW)
Short Pulse	< 6	≤ 800	60 - 150	100	≥ 7
Low Rep. Rate	<250	25	60 - 150	16	≥ 1
High Power	Any	≤ 800	60 - 150	1000	≤ 45
Low Power	0 to ≥25	1 to 800	10 - 20	0-10000	Any

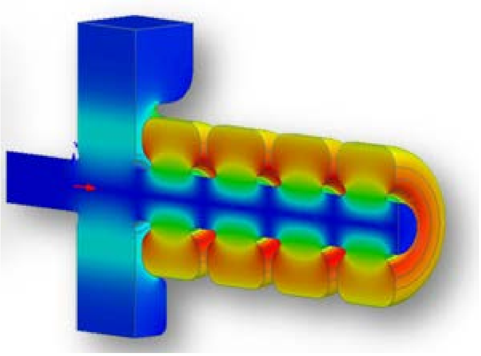

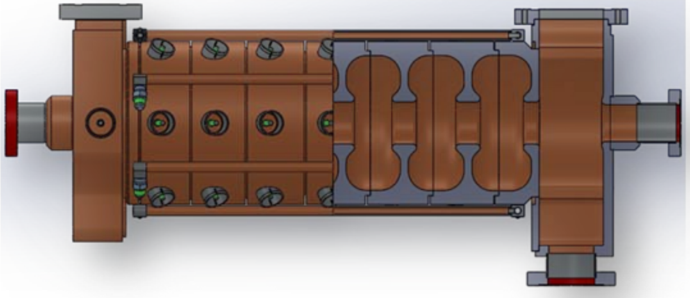

Measurement Capabilities at the RPI LINAC

- **Thermal Region:** Transmission, Capture, Fission
- **Resolved Resonance Region**: Transmission, Capture, Fission
- **Unresolved Resonance Region**: Transmission, Capture, Fission
- **Fast Neutrons**: Transmission, Scattering, Prompt Fission Neutron Spectrum
- **Lead Slowing Down Spectrometer**: Fission, (n, alpha), (n, p), Capture

Nuclear Data are used in Reactor Design

Reactor Physics Calculations

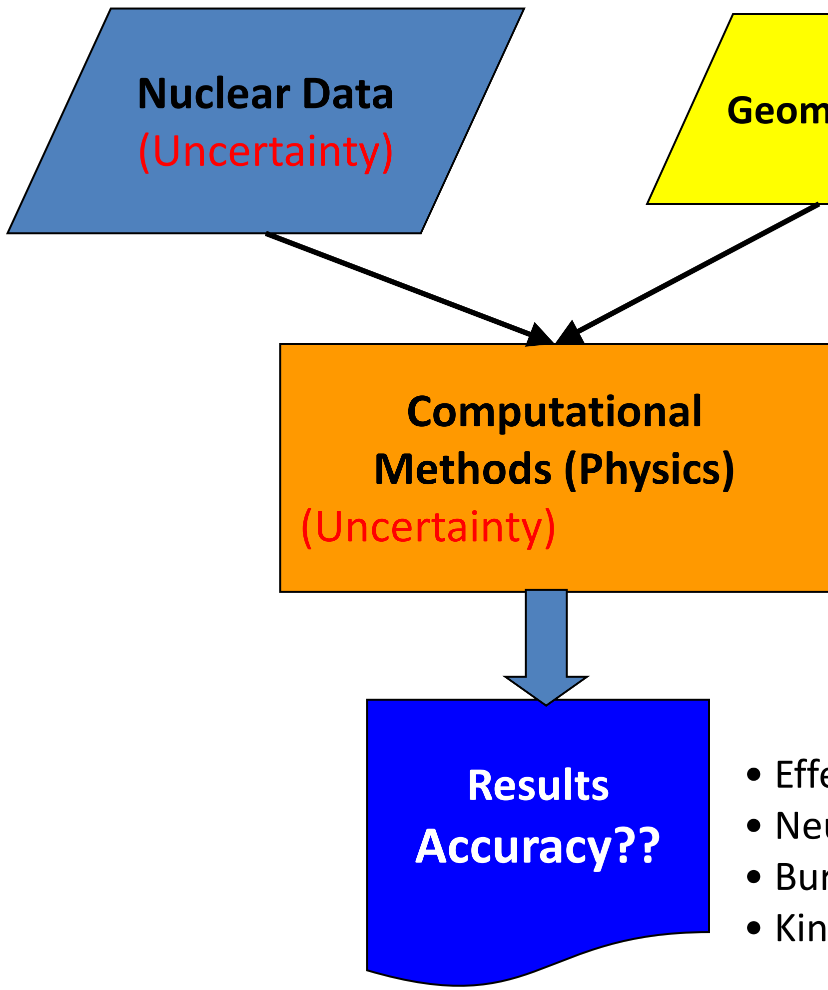

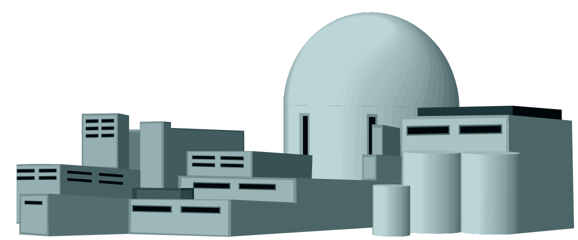

- Effective neutron Multiplication factor
- Neutron flux
- Burnup
- Kinetics

Nuclear Reactor Design Limitations

- Modern computational methods are greatly improved
- Monte Carlo Methods
  - Advantages
    - Can describe the geometry at a level of a CAD drawing.
    - Includes different physics models in great detail.
    - Can solve time dependent problems.
  - Limitations
    - **Accuracy is limited by Nuclear Data and Physics models**
    - Slow for some types of calculations (but computers are getting faster)

Nuclear Reaction Cross Section

- The cross section represents the probability for neutron interaction and is measured in units of area.

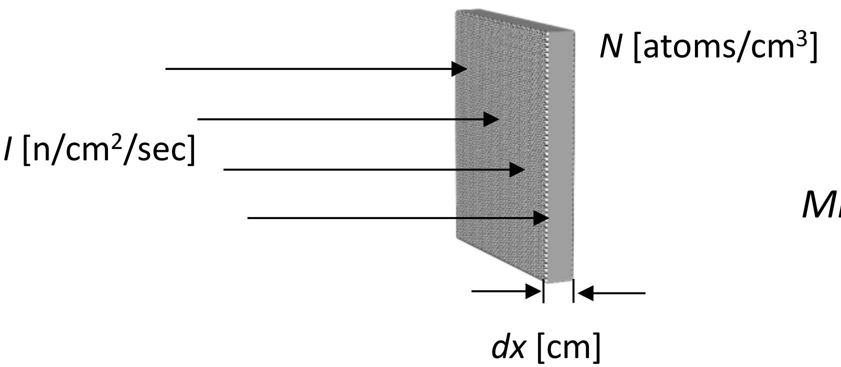

Microscopic cross section

$$R\left[\frac{\#}{\text{sec}}\right] = I\left[\frac{n}{cm^2 \cdot \text{sec}}\right] \cdot N\left[\frac{atoms}{cm^3}\right] \cdot \sigma\left[\frac{cm^2}{atom}\right] \cdot A\left[cm^2\right] \cdot dx\left[cm\right]$$

Probability for interaction $= \dfrac{\text{Reaction rate}}{\text{Incident particle rate}} = \dfrac{IN\sigma A dx}{AI} = N\sigma dx$

Why parameterize the resonances?

- **Parametrization advantages:**
  - Enables temperature (Doppler) broadening
  - Save space
  - Preserves unitarity
  - Enables evaluations of experimental data.

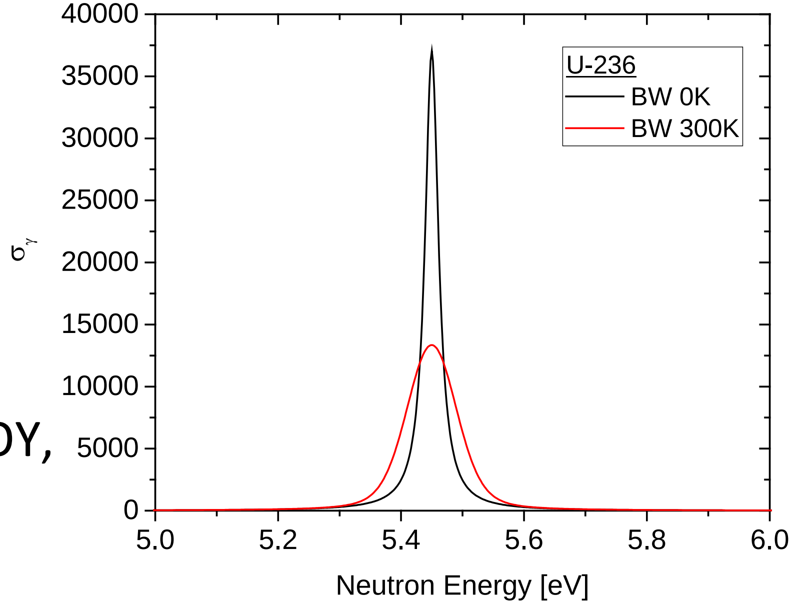

- Use resonance analysis codes
  - SAMMY (ORNL)
  - REFIT (Moxon, UK)
  - CONRAD (NEA, France)
- Reconstruct the cross section using, NJOY, AMPX , etc.

Are We Improving Reactor Calculations ?

Feedback of the new RPI Gd resonance parameters set on FUBILA Full MOX poisoned core calculation

P. Blaise – O. Litaize
Reactor Physics and Cycle Service (SPRC\LEPh)

CADA

NUCLEAR SCIENCE AND ENGINEERING: **163**, 17–25 (2009)

Impact of New Gadolinium Cross Sections on Reaction Rate Distributions in 10 × 10 BWR Assemblies

G. Perret,* M. F. Murphy, and F. Jatuff†
Paul Scherrer Institut, CH-5232 Villigen PSI, Switzerland

J-Ch. Sublet and O. Bouland
Commissariat à l'Energie Atomique, DEN, Cadarache, 13108 St Paul lez Durance, France

and

R. Chawla
Paul Scherrer Institut, CH-5232 Villigen PSI, Switzerland
and
École Polytechnique Fédérale de Lausanne, CH-1015 Lausanne, Switzerland

Received July 28, 2008

...on (C_8/F_{tot}) ...OTEUS pro- ...e measured ... ratios were ...e effort was ...out success. ...y Leinweber et al. and differed significantly from current library values. ENDF/B-VII.0 gadolinium cross sections have currently been modified to include the new measurements, and these data have been processed with NJOY to yield files usable by MCNPX. Fission rates in the gadolinium-poisoned fuel pins of the SVEA-96 Optima2 pins were increased by 1.4 to 2.0% using the newly produced cross sections, yielding to a better agreement with the experimental values. Predicted C_8/F_{tot} ratios were decreased on average by 1.7% in both clustered and unclustered groups of gadolinium-poisoned fuel pins of the SVEA-96+ assembly correcting the overpredictions previously reported in the clustered gadolinium pins. Earlier reported discrepancies observed in PROTEUS integral experiments, between measured and calculated reaction rates in the gadolinium-poisoned pins, might thus be due to inaccurate gadolinium cross sections. The PROTEUS results support the new thermal and epithermal gadolinium data measured by Leinweber et al.

correcting the overpredictions previously reported in the clustered gadolinium pins. Earlier reported discrepancies observed in PROTEUS integral experiments, between measured and calculated reaction rates in the gadolinium-poisoned pins, might thus be due to inaccurate gadolinium cross sections. The PROTEUS results support the new thermal and epithermal gadolinium data measured by Leinweber et al.

Resonance Cross Section Measurements Data Analysis

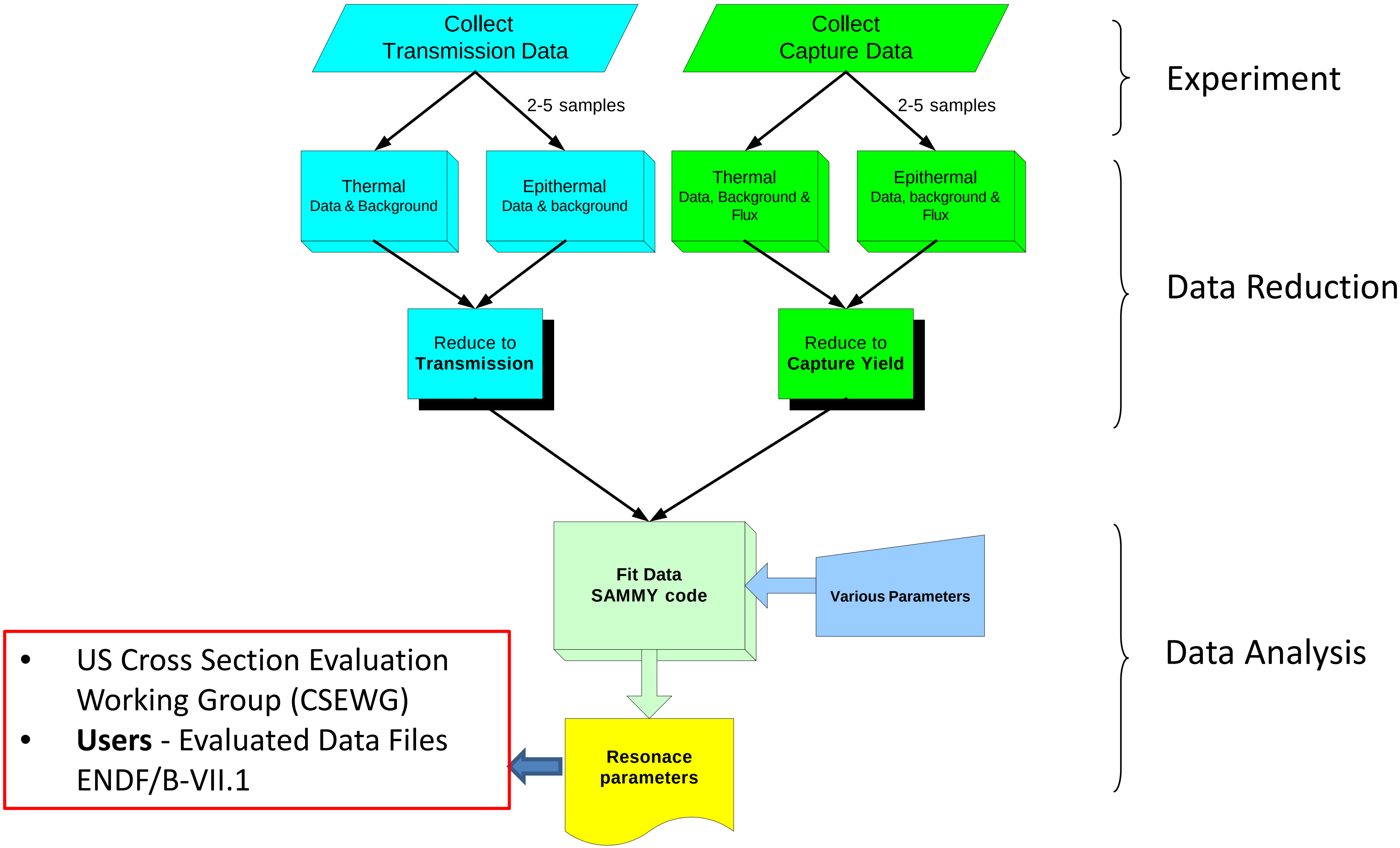

Cadmium as a Neutron Absorber

Total Thermal Cross Section ~20000 barns

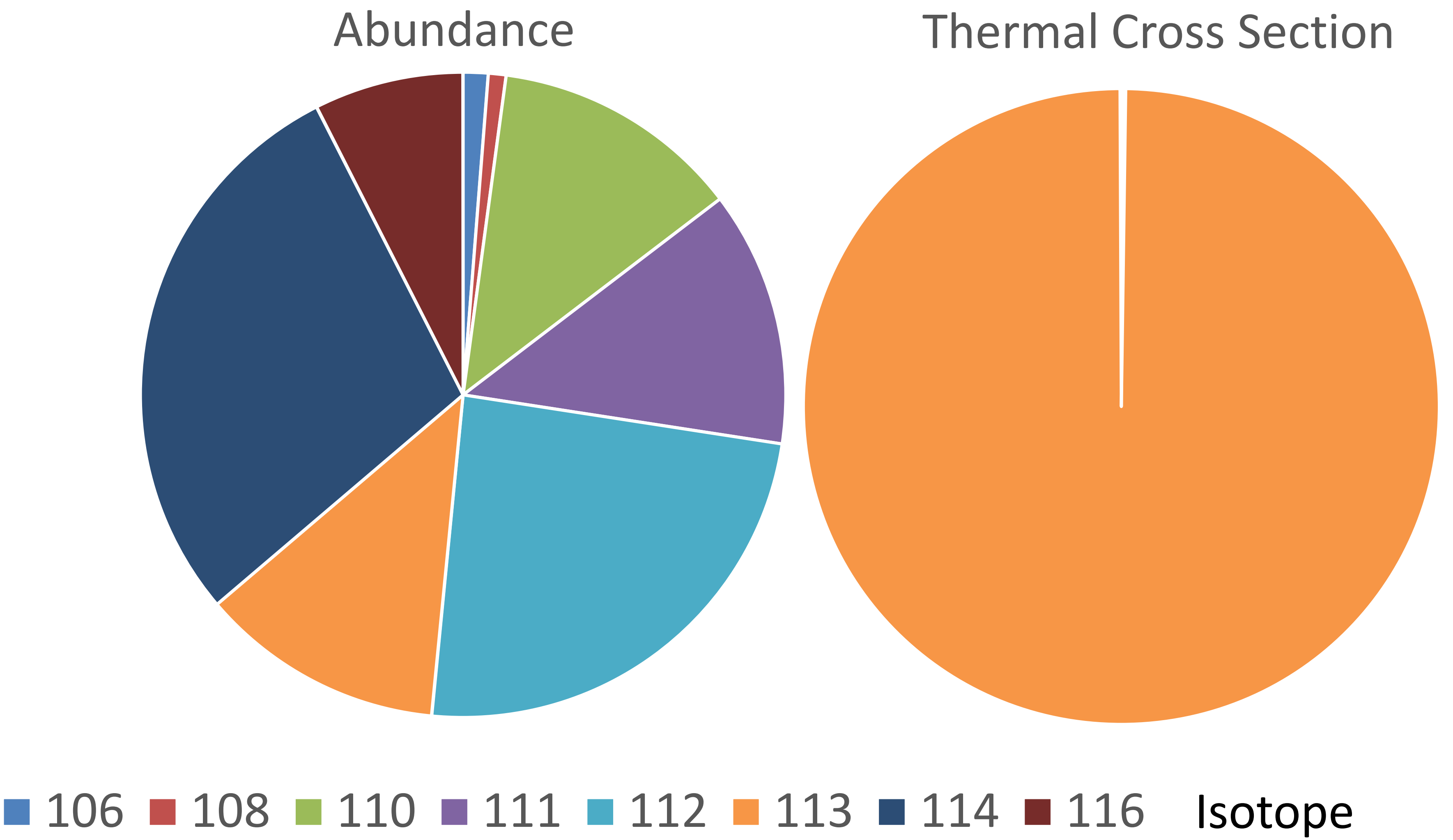

Neutron Production

1. Bremsstrahlung X-rays are produced by stopping the electrons.
2. The X-rays produce neutrons by (γ,n).

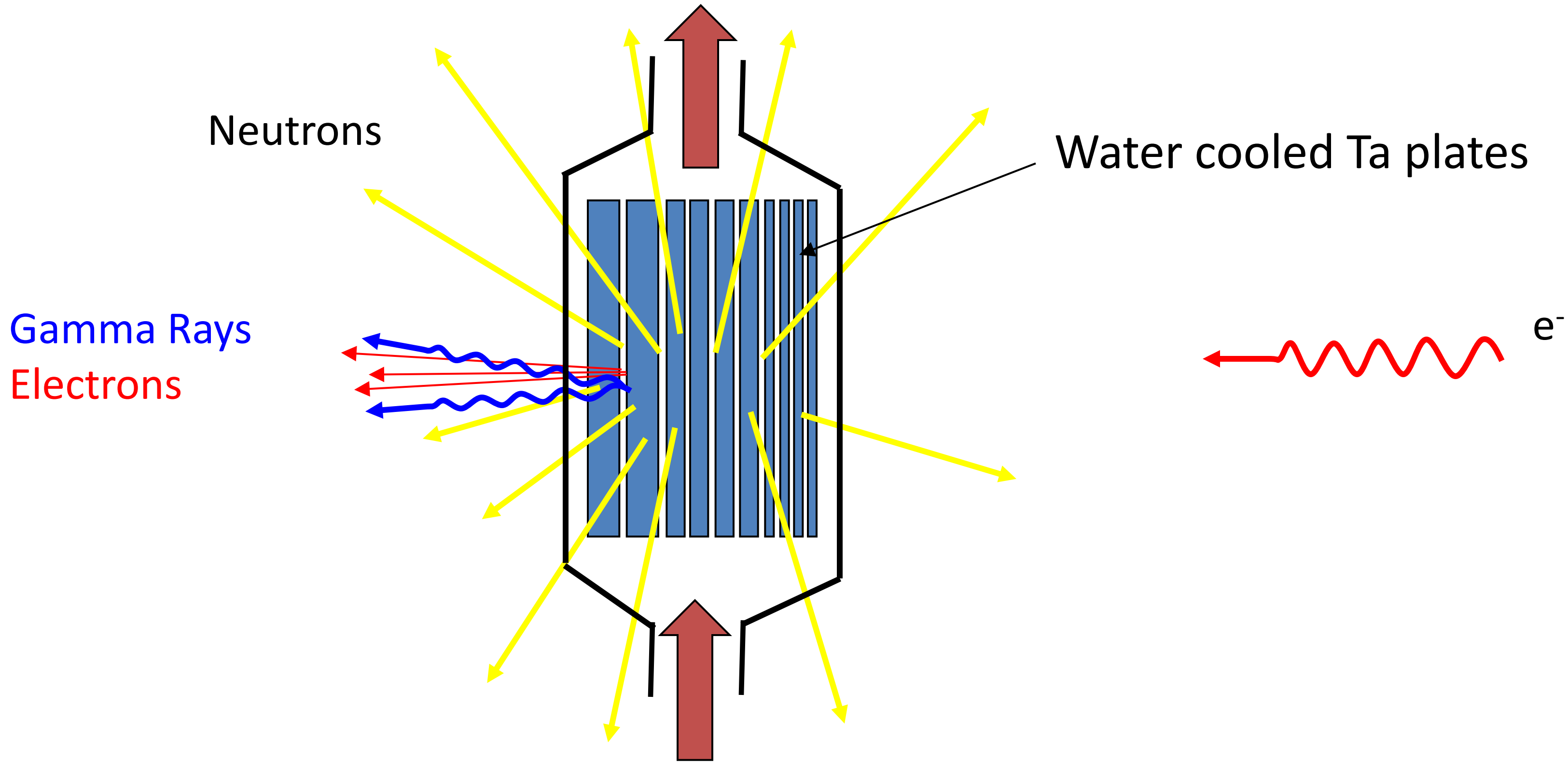

Neutron-Producing Targets

Enhanced thermal target

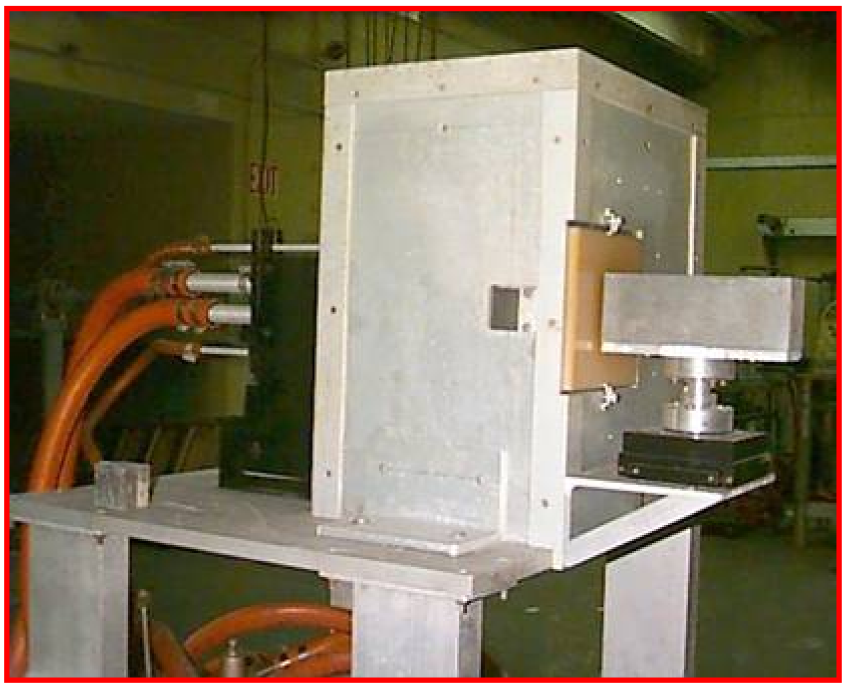

Bare bounce target

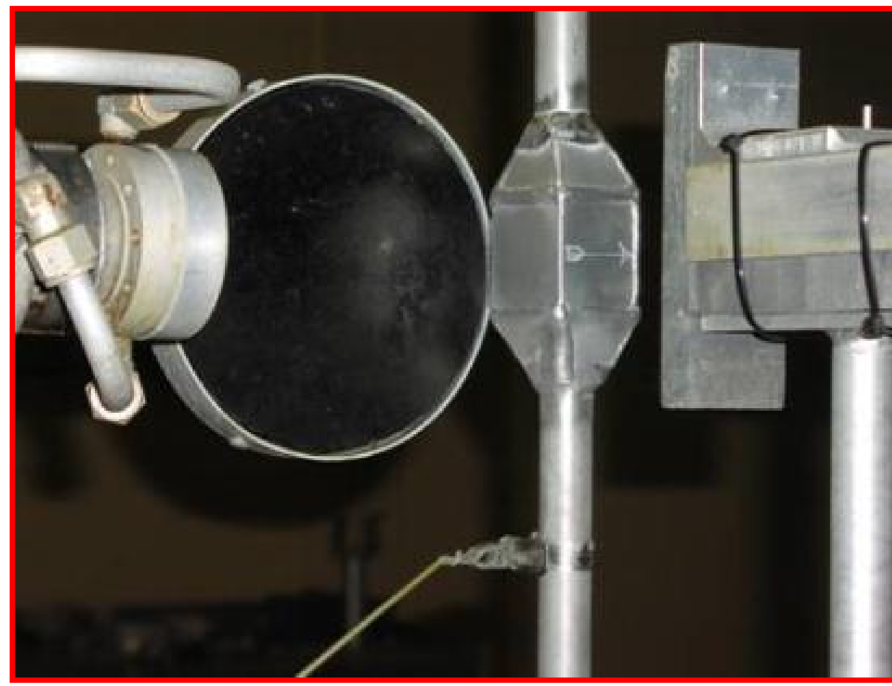

Time of Flight (TOF)

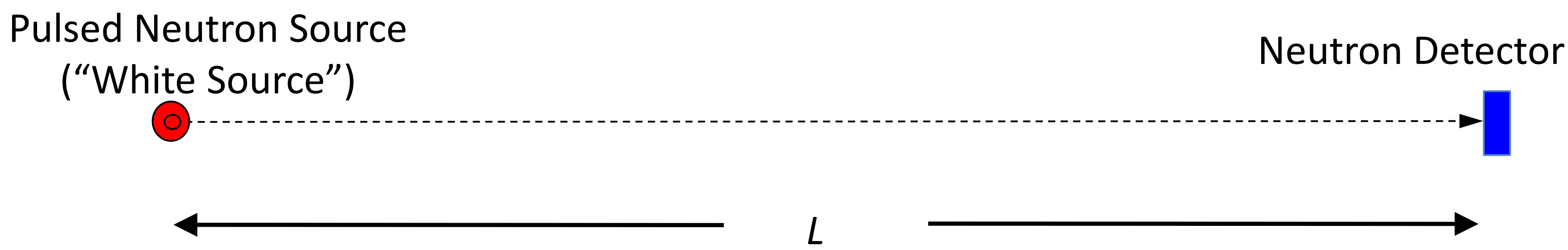

Energy-Time relation (nonrelativistic)

$$v = \frac{L}{t} \quad , \quad E = \frac{1}{2} m \cdot v^2 \Longrightarrow E = \left(\frac{K \cdot L}{t - t_0} \right)^2$$

K - constant
t_0 - time zero (gamma flash)

- **Energy Resolution**
  - Related to:
    - ΔL/L – moderator + detector
    - Δt/t – LINAC electron pulse

Transmission Experiment

Two Experiments:

1. Sample Out

Neutron Beam

Li-Glass Neutron Detector

2. Sample In

Neutron Beam

Sample

Li-Glass Neutron Detector

$$T = \frac{C_{\text{Sample In}}}{C_{\text{Sample Out}}} = \exp(-N\sigma_t)$$

N – Number density [atoms/barn]

σ_t – Total cross section

C – Counting rate

Epithermal Transmission Experimental Setup

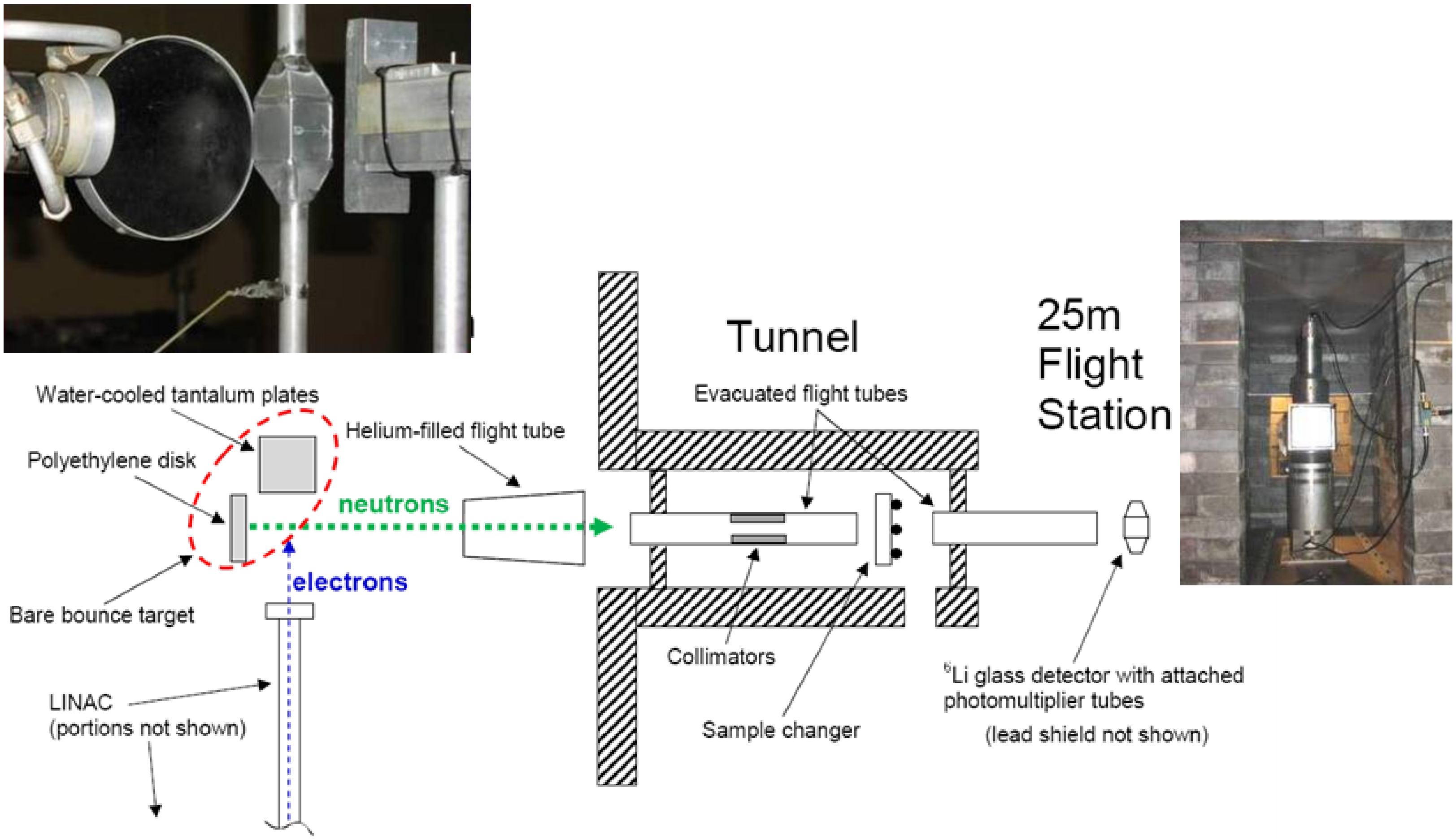

Capture Experiments

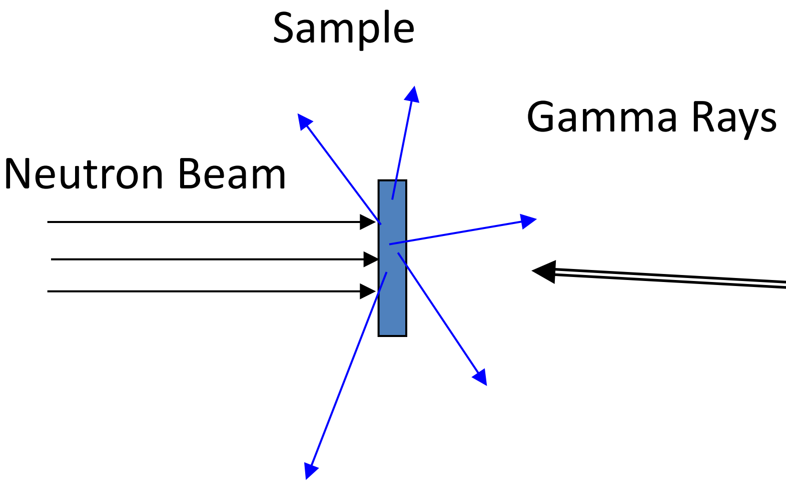

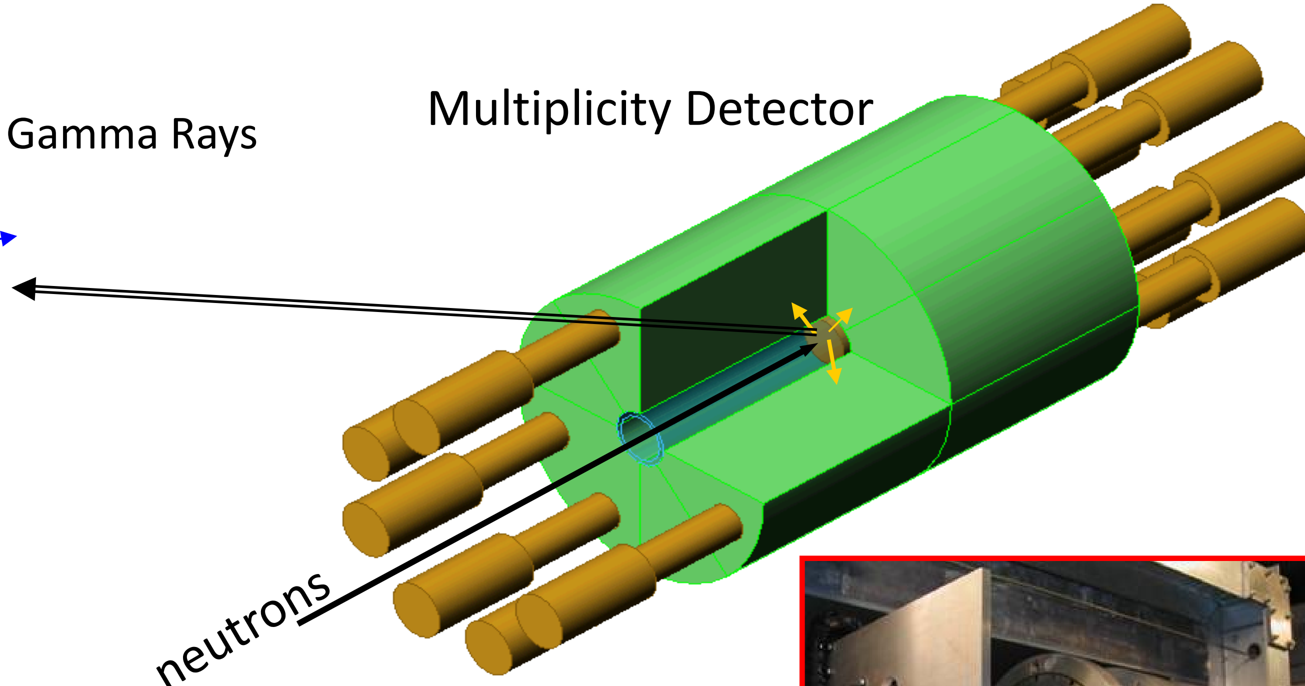

The capture Yield:

ϕ – neutron flux

η – detection efficiency

$$Counts = \phi Y \eta$$

$$Y = \left(1 - \exp(-N\sigma_t)\right)\frac{\sigma_\gamma}{\sigma_t}$$

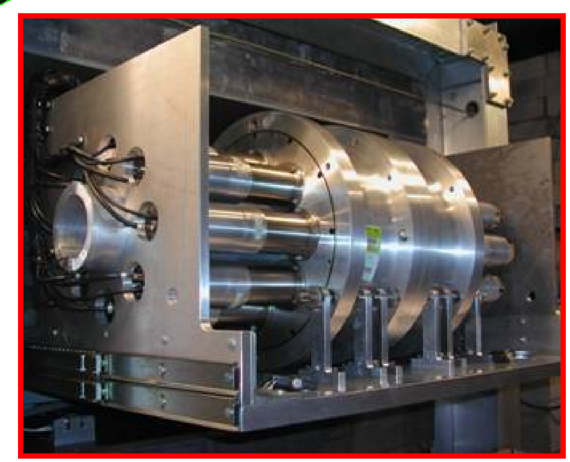

Highlights of the Cadmium Resonance Region Measurements

- Multiple samples, transmission and capture, thermal and epithermal
  - Consistency among data sets provides confidence in common results.
- Background in transmission determined from separate "notch filter" runs to get the background shape
  - Normalized to a "fixed" notch
- Used the JENDL values for the negative energy resonances
  - No negative energy resonance for Cd113 and none needed
  - All other resonances are of secondary value with regards to fitting the thermal cross section.
- Nuclear radii fit well
  - Data support a small adjustment in the Cd113 radius
  - Radii were fitted between resonances

Thermal Cd Measurements

	^{113}Cd	
	Thermal Capture Cross Section (barns)	Capture Resonance Integral (barns)
NNL/RPI	20051 ± 14	383 ± 1
ENDF/B-VII.1	19862	384
JEFF-3.2	20165	400
JENDL-4.0	20062	387

	NNL/RPI	ENDF/B-VII.1
Energy (eV)	0.1779 ± 0.0002	0.1787
Γ_n (meV)	0.638 ± 0.008	0.6336
Γ_γ (meV)	112.4 ± 0.4	113.5

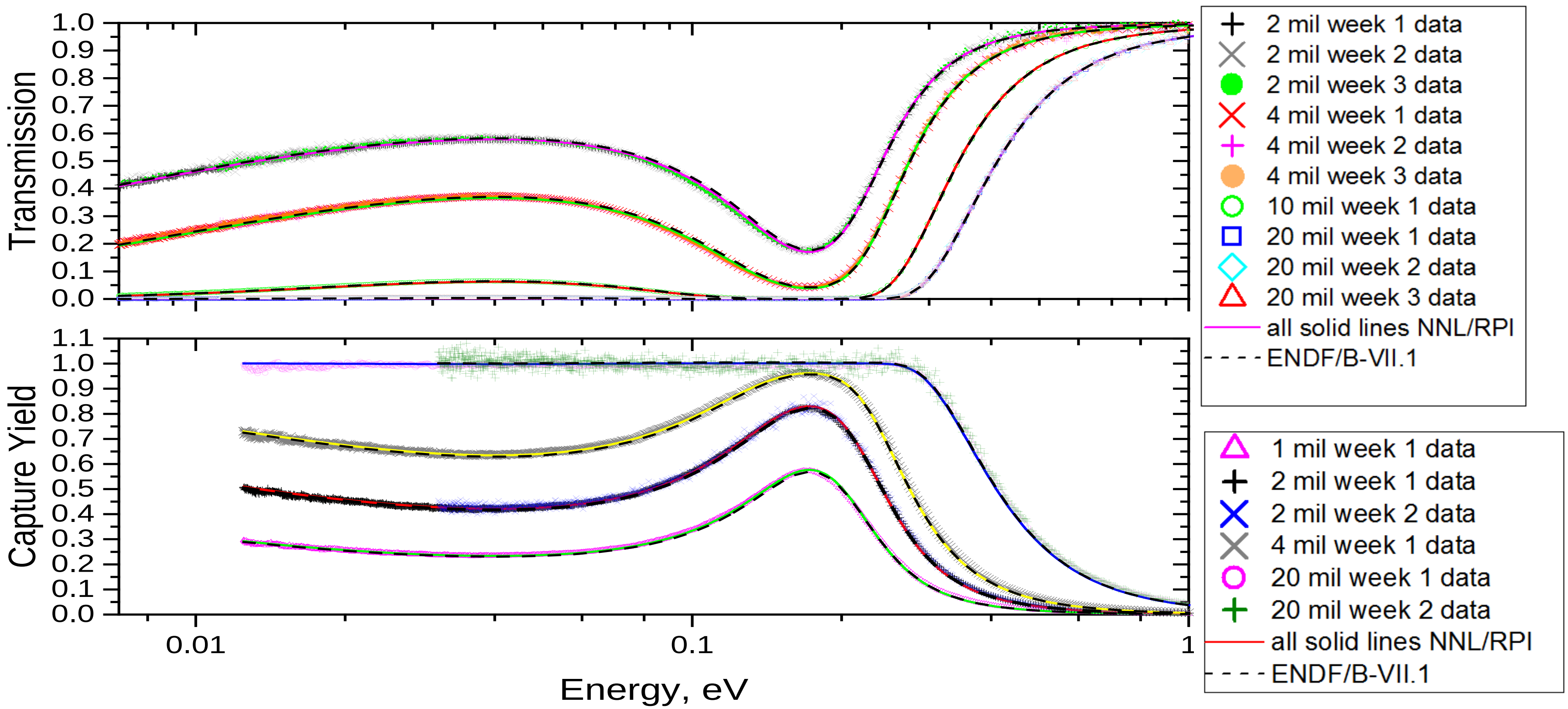

Historical Evaluations of the Cd 0.178 eV resonance

$$\sigma_{tot}\ \alpha\ \frac{\Gamma_n}{\Gamma_n + \Gamma_\gamma}$$

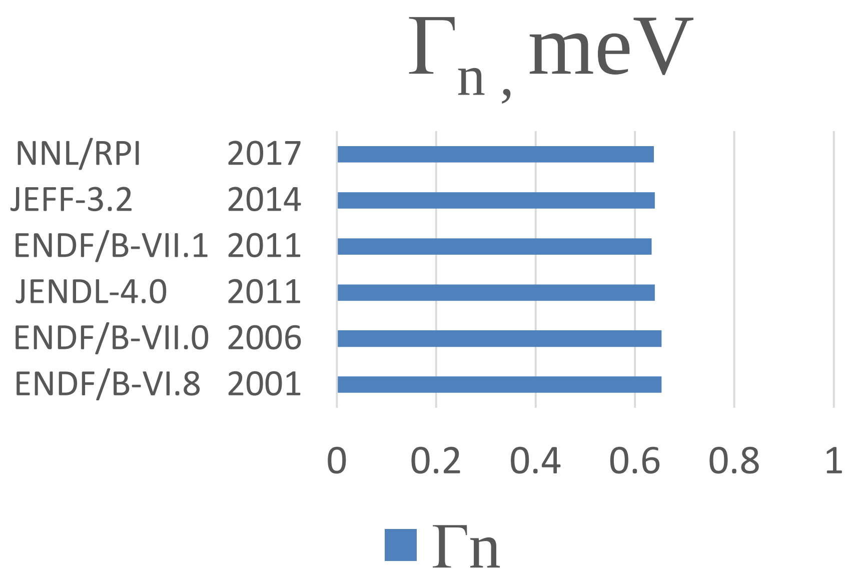

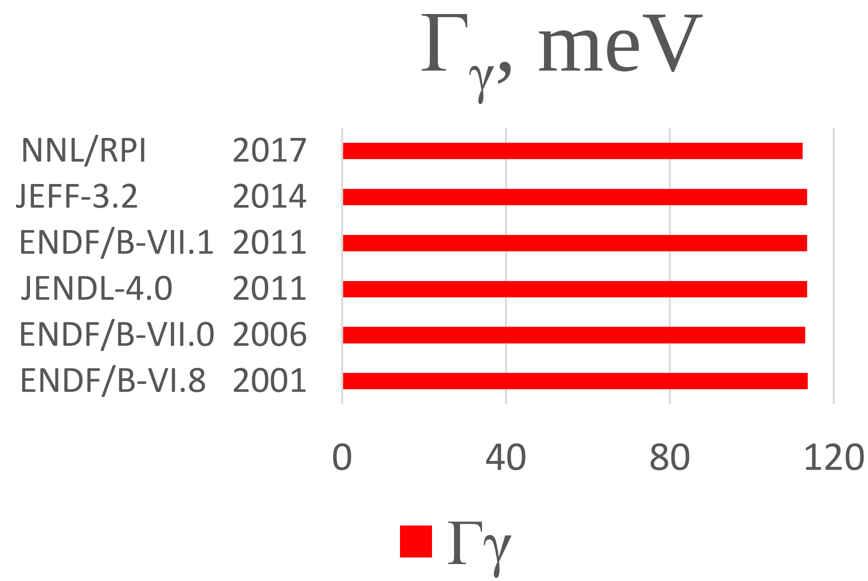

Source	Energy, eV	Γ_γ, meV	Γ_n, meV	Date
NNL/RPI	0.1779	112.4 ± 0.4	0.638 ± 0.008	2017
JEFF-3.2	0.1787	113.5	0.64	2014
ENDF/B-VII.1	0.1787	113.5	0.63362	2011
JENDL-4.0	0.1787	113.5	0.64	2011
ENDF/B-VII.0	0.178	113	0.65333	2006
ENDF/B-VI.8	0.178	113.65	0.65333	2001

Historical Measurements of the Cd 0.178 eV resonance

$$\sigma_{tot} \; \alpha \; \frac{\Gamma_n}{\Gamma_n + \Gamma_\gamma}$$

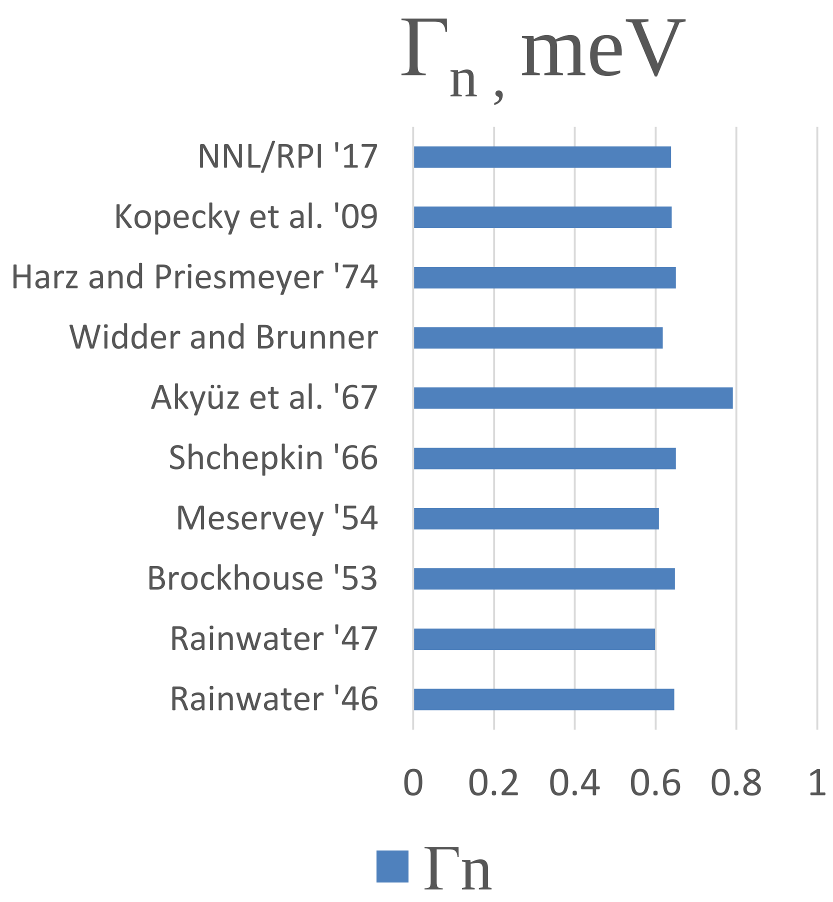

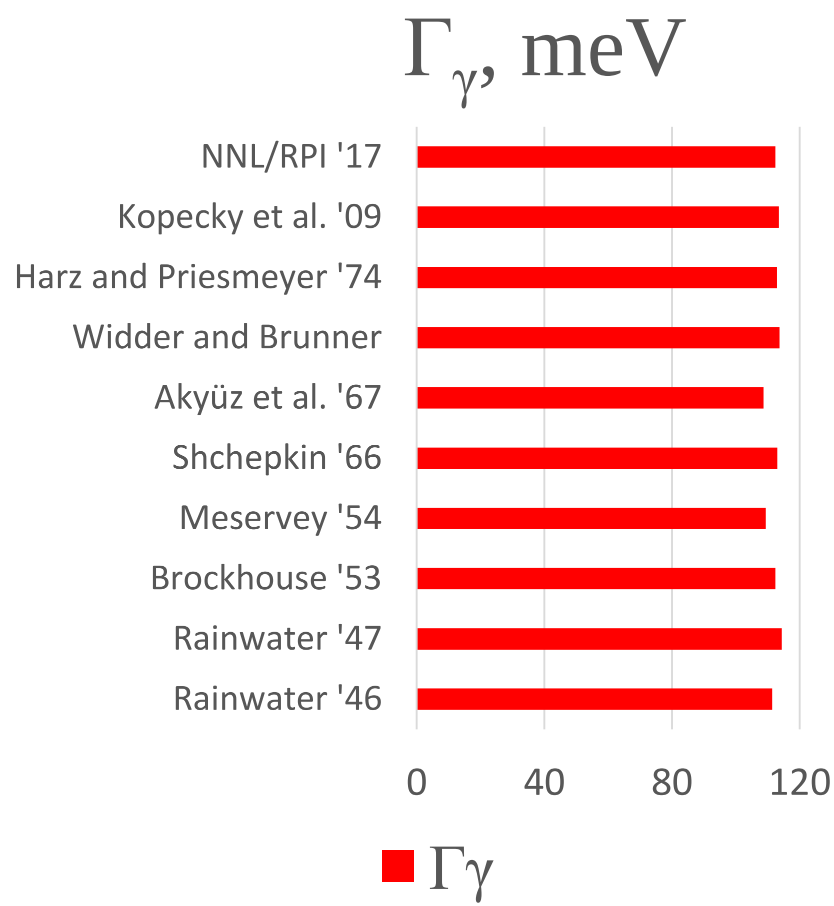

^{113}Cd Strength Functions

$$S_0 = \frac{\langle \Gamma_n^0 \rangle}{\langle D \rangle}$$, where $\langle \Gamma_n^0 \rangle$ is the average reduced neutron width, and $\langle D \rangle$ is the average level spacing for s-wave resonances

Source	Neutron Strength Function in units of 10^{-4}
NNL/RPI	0.35 ± 0.06
JEFF-3.2	0.33 ± 0.07
ENDF/B-VII.1	0.35 ± 0.06
JENDL-4.0	0.35 ± 0.07
ENDF/B-VII.0	0.35 ± 0.06
Atlas 2006	0.44 ± 0.06
ENDF/B-VI.8	0.33 ± 0.10
Atlas 1981	0.31 ± 0.07

Cadmium Experimental Details

<table>
<tr><th>Experiment</th><th>Overlap Filter</th><th>Neutron-Producing Target</th><th>Electron Pulse Width (ns)</th><th>Ave. Beam Current (μA)</th><th>Beam Energy (MeV)</th><th>Pulse Repetition Rate (pulses/s)</th><th>Flight Path Length (m)</th><th>Normalization Point for Transmission Background or Capture Flux (eV)</th></tr>
<tr><td>Epithermal Transmission</td><td>Boron Carbide</td><td>Bare Bounce</td><td>53</td><td>22</td><td>56</td><td>225</td><td>25.589 ± 0.007</td><td>45 eV resonance in Mo95 fixed notch</td></tr>
<tr><td>Thermal Transmission Week 1 of 3</td><td rowspan="3">None</td><td rowspan="3">Enhanced Thermal Target</td><td>1875</td><td>12</td><td>50</td><td rowspan="3">25</td><td rowspan="3">14.973 ± 0.004</td><td>18.8 eV resonance in W186</td></tr>
<tr><td>Thermal Transmission Week 2 of 3</td><td>920</td><td>6</td><td>55</td><td rowspan="2">5.2 eV resonance in Ag109</td></tr>
<tr><td>Thermal Transmission Week 3 of 3</td><td>900</td><td>6</td><td>60</td></tr>
<tr><td>Epithermal Capture</td><td>Boron Carbide</td><td>Bare Bounce</td><td>≈49</td><td>23</td><td>54</td><td>225</td><td>25.564 ± 0.006</td><td>27 eV resonance in Cd111 in the 200-mil sample</td></tr>
<tr><td>Thermal Capture</td><td>None</td><td>Enhanced Thermal Target</td><td>1400</td><td>11</td><td>50</td><td>25</td><td rowspan="2">25.444 ± 0.004</td><td rowspan="2">0.178 eV resonance in Cd113 in 20-mil sample data</td></tr>
<tr><td>Thermal Capture</td><td>None</td><td>Enhanced Thermal Target</td><td>770</td><td>8.5</td><td>54</td><td>25</td></tr>
</table>

Transmission data for Cd

- Sample-in and open beam data before forming transmission fraction
- Includes fixed molybdenum “notch” at 45 eV
- Many more resonances in the Cd sample data

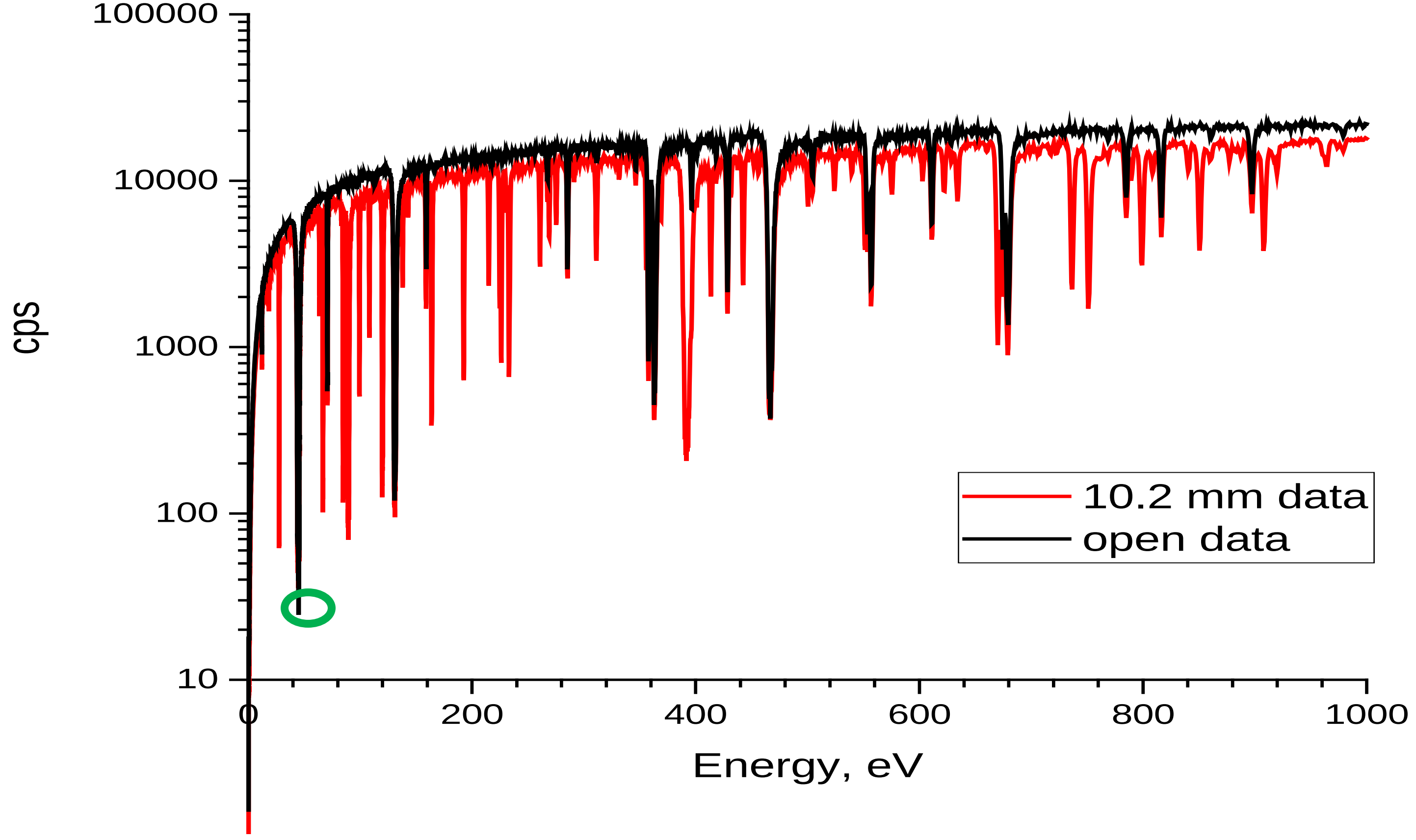

Transmission Background Methods

- Use Notch 0 ≈ (Notch 1)^2/Notch 2
  - normalized to a fixed notch
    - Use of fixed notch normalization reduces the uncertainty in the notch extrapolation method

Transmission Background Method: Notch Extrapolation

- Open beam data from Cd thermal transmission measurement
- Notch package measurements include Cd, In, Ag, and W, and normalized at W

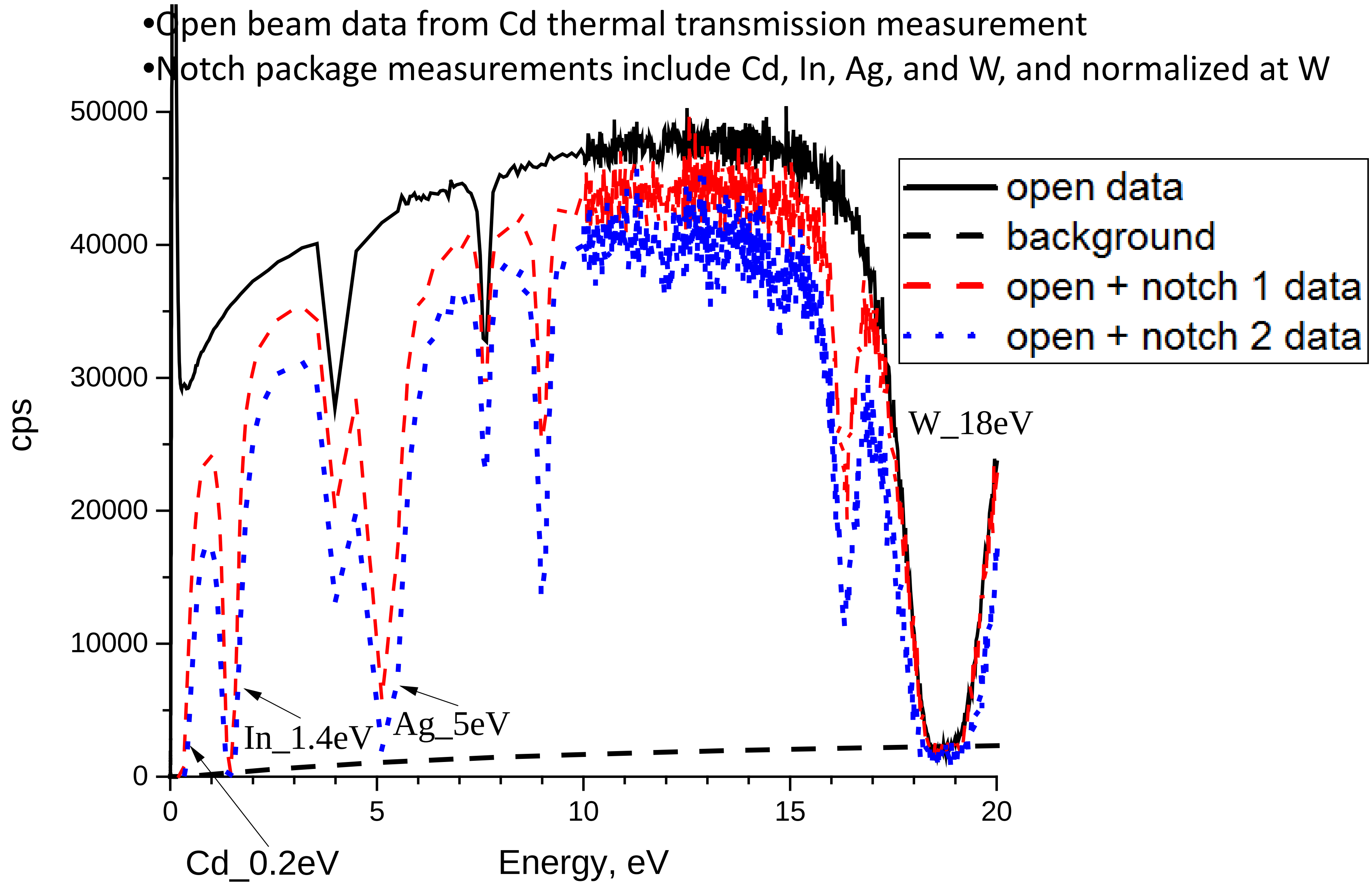

Thermal Cd Signal-to-Background

Open Beam data and transmission background

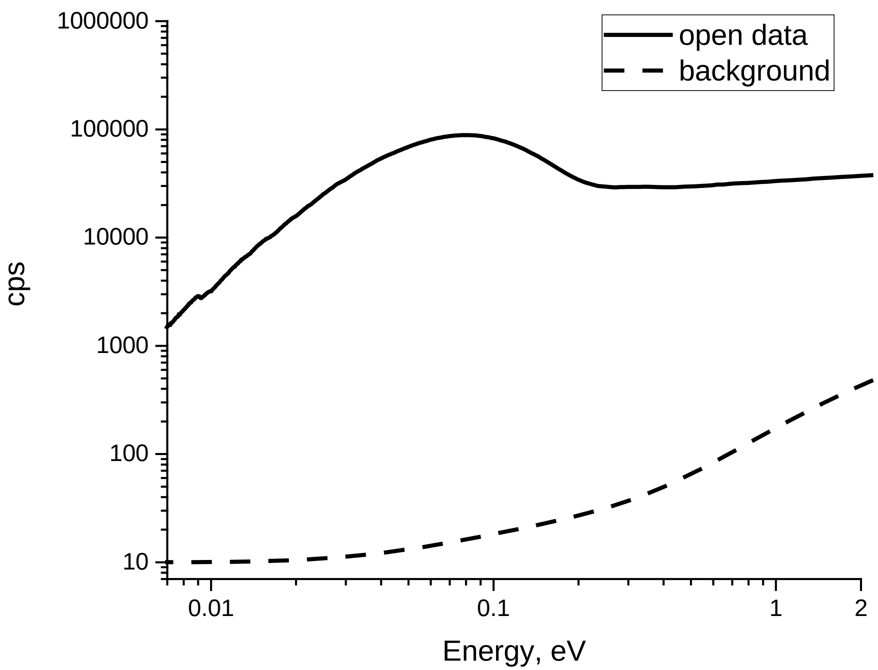

Signal-to-Background Ratio

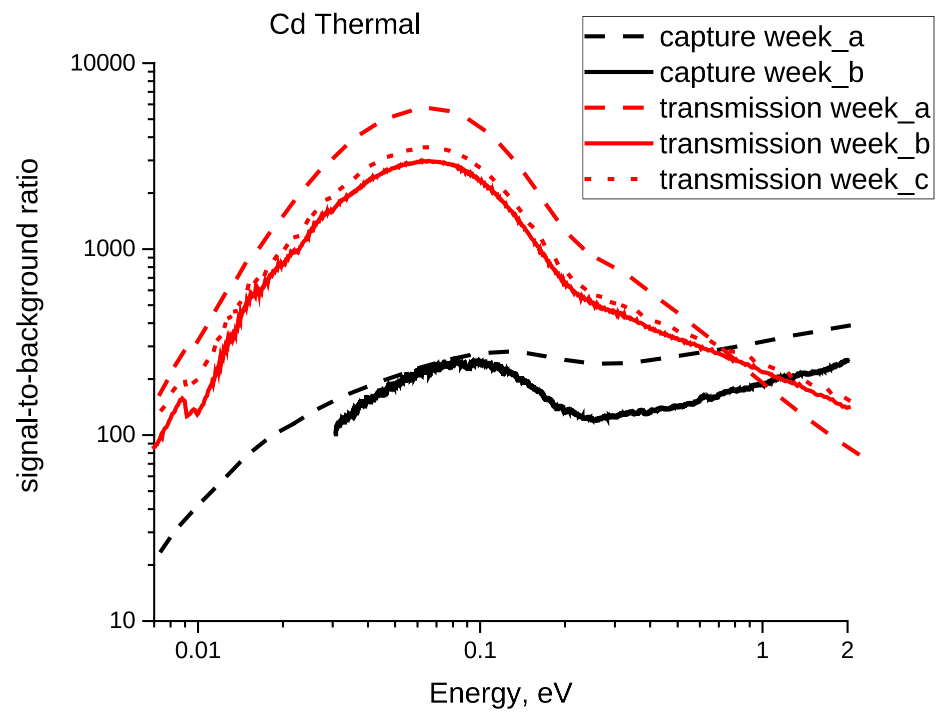

Epithermal Cd Signal-to-Background

Open Beam with Fixed Mo Notch and transmission background

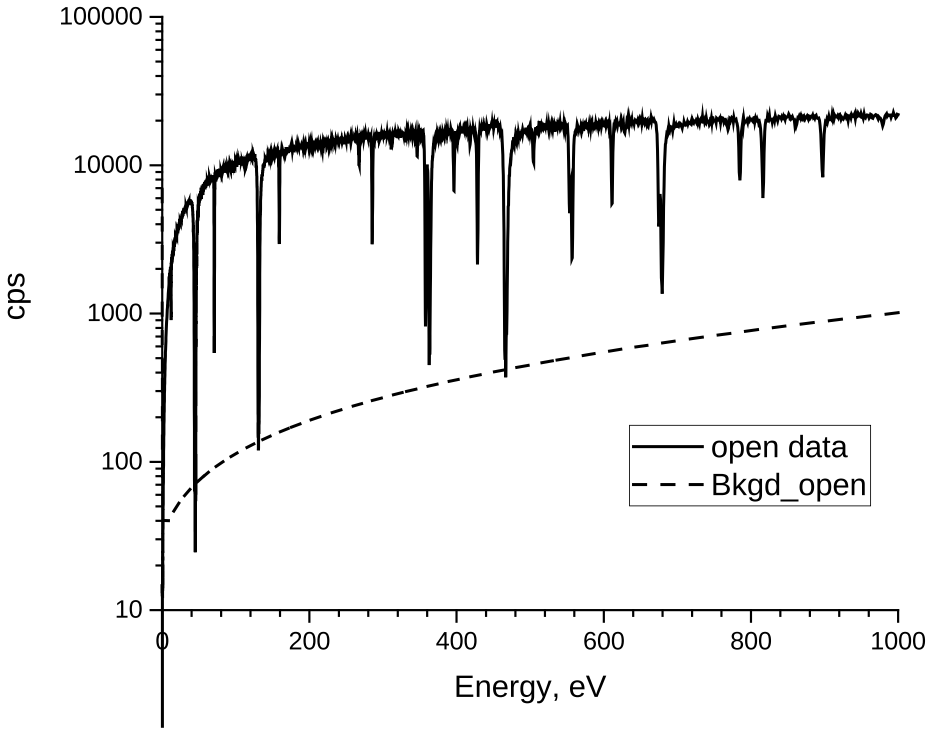

Signal-to-Background Ratio

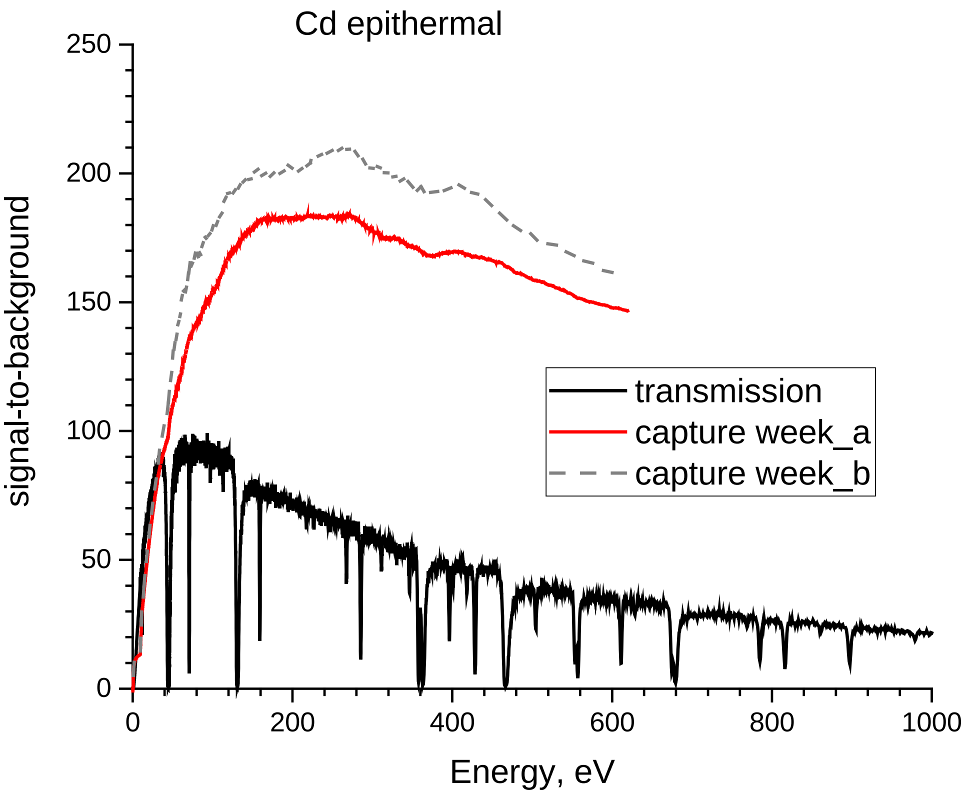

Cd 0.178 eV Resonance

	NNL/RPI	ENDF/B-VII.1	JEFF-3.2	JENDL-4.0
Energy (eV)	0.1779 ± 0.0002	0.1787	0.1787	0.1787
Γ_n (meV)	0.638 ± 0.008	0.6336	0.64	0.64
Γ_γ (meV)	112.4 ± 0.4	113.5	113.5	113.5

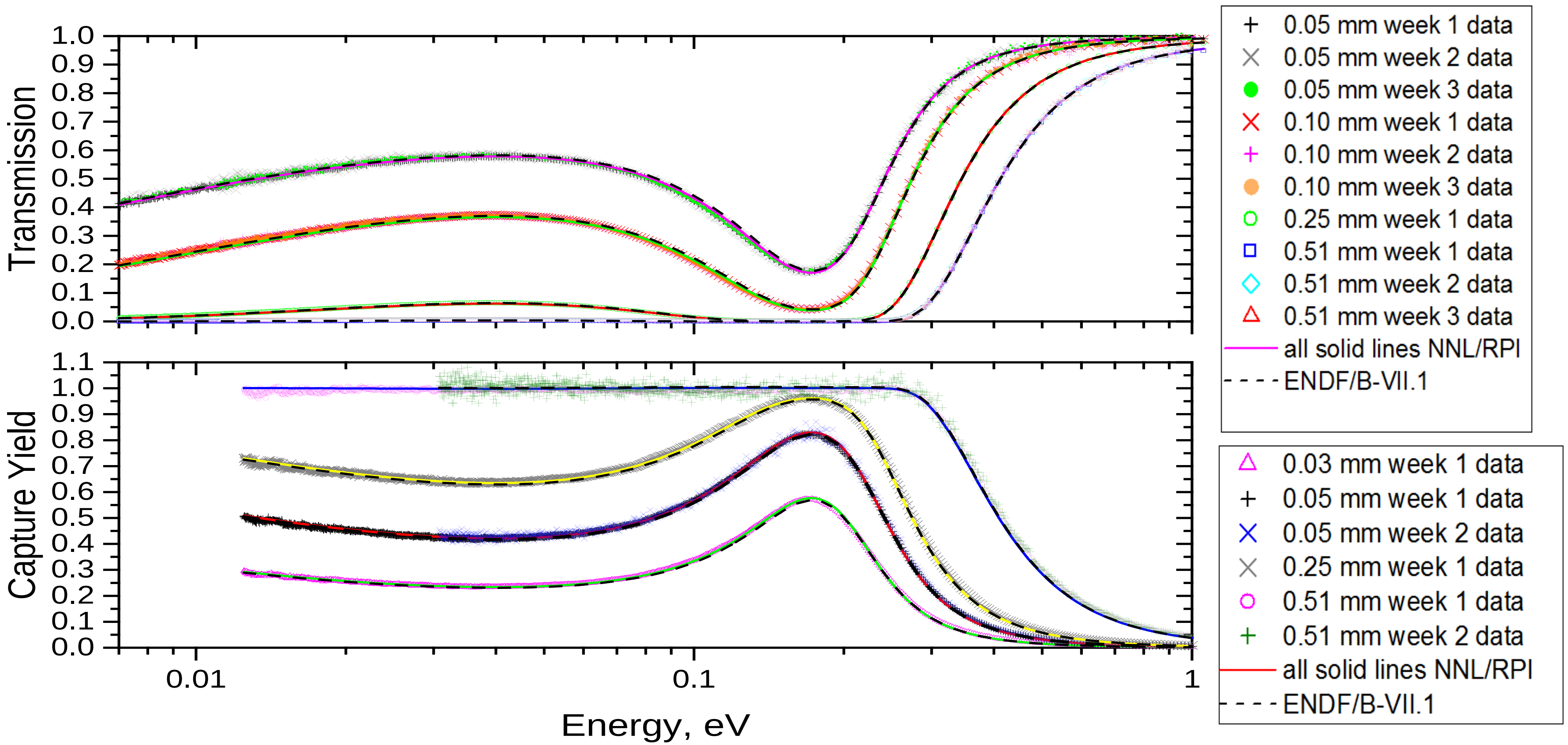

Cadmium Resonance Region up to 1 keV

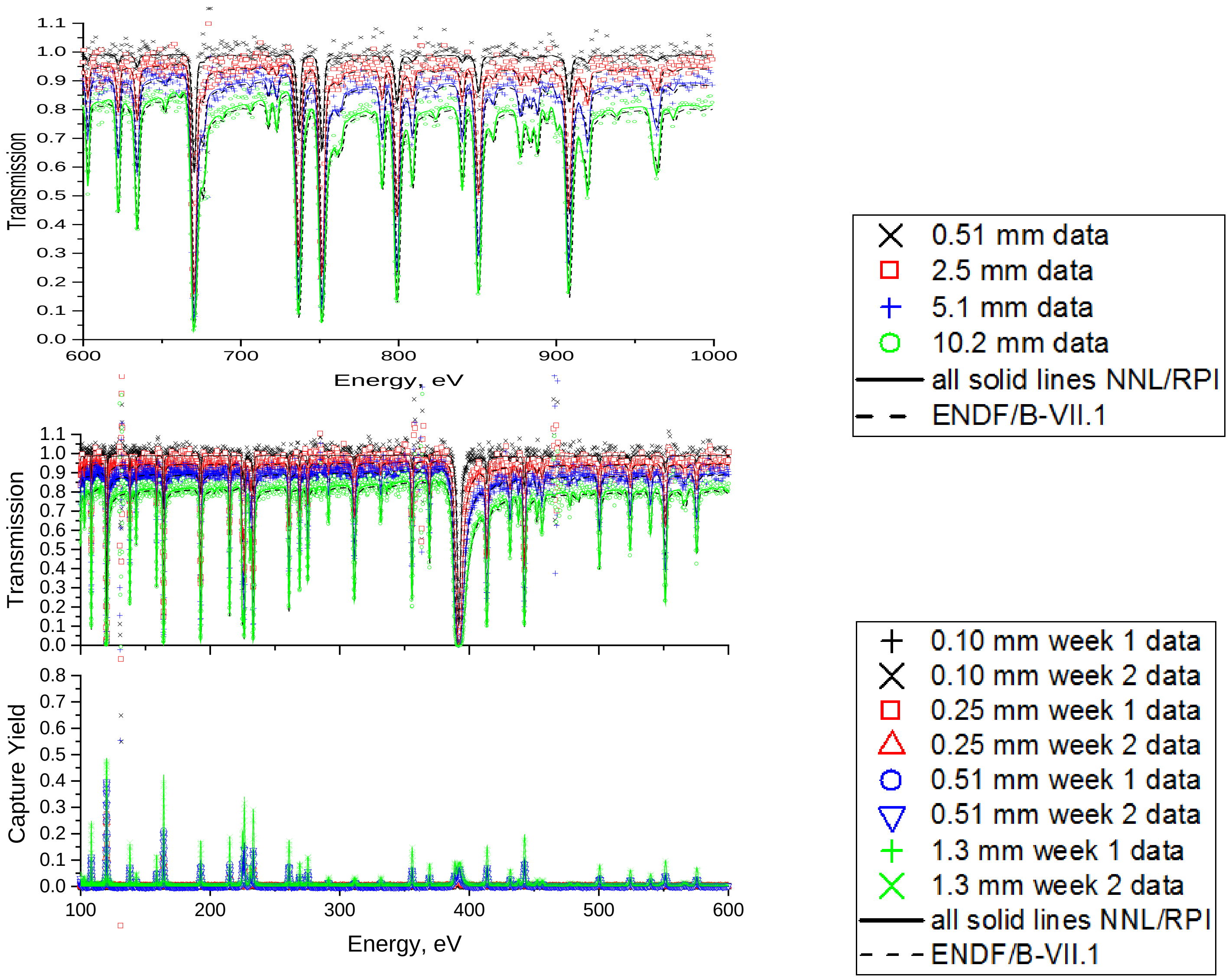

Account for Differences Between Data Sets External Uncertainties

- X refers to either E_R, Γ_n, or Γ_γ
- The subscripts B and ext refer to final Bayesian uncertainties and external uncertainties

$$< X >_{ext} = \left. \sum_1^n \frac{X_i}{(\Delta X_{B,i})^2} \middle/ \sum_1^n \frac{1}{(\Delta X_{B,i})^2} \right.$$

$$\Delta X_{ext} = \sqrt{\left\{ \sum_1^n \frac{(X_i - < X >_{ext})^2}{(\Delta X_{B,i})^2} \right\} / \left\{ (n-1) \sum_1^n \frac{1}{(\Delta X_{B,i})^2} \right\}}$$

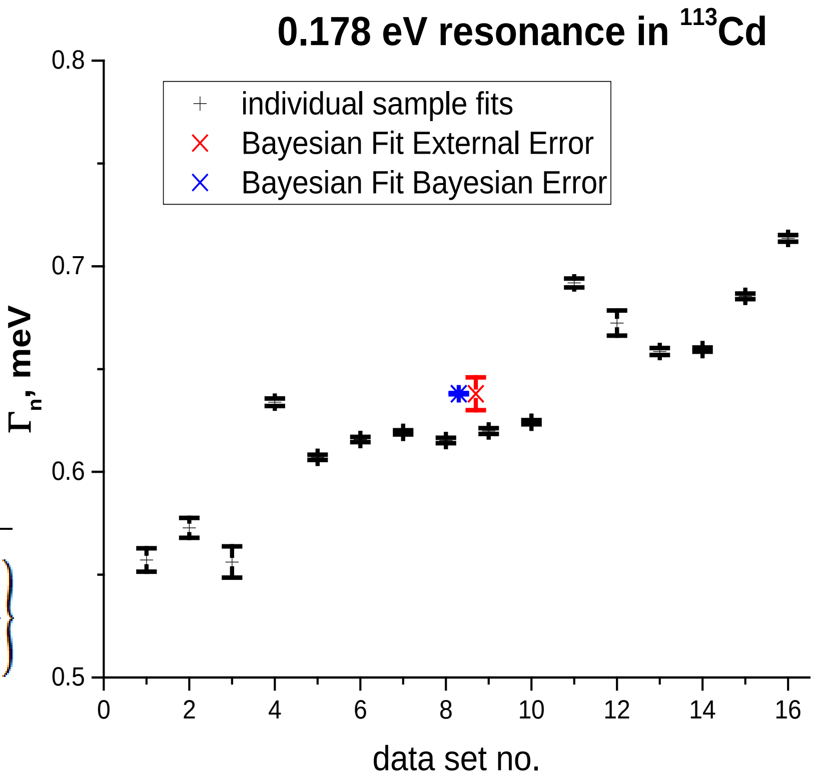

Conclusions

- Multiple measurements of Cd were performed in the resolved resonance region
- Thermal cross sections
  - Current results similar to ENDF/B-VII.1, JEFF-3.2, and JENDL-4.0, closest to JENDL-4.0
- Capture resonance integrals
  - Current results similar to ENDF/B-VII.1, JEFF-3.2, and JENDL-4.0, closest to JEFF-3.2, and JENDL-4.0
- RPI LINAC 2020 refurbishment and upgrade
  - Ambitious project is underway and on schedule

Extra Slides

Reaction Rates

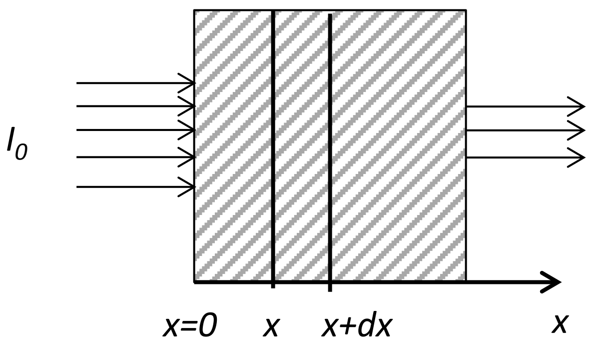

$$-dI = -\left[I(x+dx) - I(x)\right] = N\sigma_t I dx$$

$$\frac{dI}{dx} = -N\sigma_t I(x)$$

$$I(x) = I_0 \exp(-N\sigma_t x) = I_0 \exp(-\Sigma_t x)$$

Probability that a neutron will not interact in distance *x*: $\exp(-\Sigma_t x)$

Probability that the neutron will first collide in *dx*: $p(x) = \exp(-\Sigma_t x)\Sigma_t$

Probability to interact in between *x*=a to *x*=b: $p(a,b) = \int_a^a p(x)dx = \int_a^b \exp(-\Sigma_t x)\Sigma_t dx = \exp(-\Sigma_t a) - \exp(-\Sigma_t b)$

Probability to interact in an infinite slab: $p(0,\infty) = \int_0^\infty p(x)dx = \Sigma_t \int_0^\infty \exp(-\Sigma_t x)dx = \exp(-\Sigma_t 0) - \lim_{x\to\infty} \exp(-\Sigma_t x) = 1$

The average distance a neutron travels before interacting with the sample, or the *__mean free path__*: $p(0,\infty) = \int_0^\infty p(x)xdx = \Sigma_t \int_0^\infty \exp(-\Sigma_t x)xdx = \frac{1}{\Sigma_t}$

The probability that a reaction of type *y* will occur in the interval [0,*x*],

$$p_y(0,x) = \int_0^x \exp(-\Sigma_t x)\Sigma_y dx = \Sigma_y \left(\frac{\exp(-\Sigma_t x)}{-\Sigma_t} - \frac{\exp(-\Sigma_t 0)}{-\Sigma_t} \right) = \frac{\Sigma_y}{\Sigma_t}\left(1 - \exp(-\Sigma_t x)\right)$$

Resonance Reactions

- We understand the shape of the resonances and use R-Matrix theory to fit the shape to measured data.
- A simplified example is the Breit-Wigner single-level formula:

<u>Reaction *x* where *x*=f or *x*=γ</u>

$$\sigma_x(E_c) = \sigma_0 \frac{\Gamma_x}{\Gamma}\sqrt{\frac{E_0}{E_c}}\frac{\Gamma^2}{4(E_c - E_0)^2 + \Gamma^2}$$

<u>Scattering reaction</u>

$$\sigma_s(E_c) = \sigma_0 \sqrt{\frac{E_0}{E}}\frac{\Gamma^2}{4(E - E_0)^2 + \Gamma^2}\left[\frac{\Gamma_n}{\Gamma} + \frac{4(E - E_0)}{\Gamma}\frac{R}{\lambda}\right] + 4\pi R^2$$

Where:

$$\sigma_0 = \frac{2.608x10^6}{E_0}\frac{A+1}{A}\frac{g\Gamma_n(E_0)}{\Gamma}$$

E_0- Resonance energy [eV]

Γ_x- radiation width Γ_γ or fission width Γ_f [eV]

Γ_n- neutron width [eV]

$\Gamma = \Gamma_\gamma + \Gamma_f + \Gamma_n$ [eV]

A – Atomic mass

g – Statistical factor (spin factor)

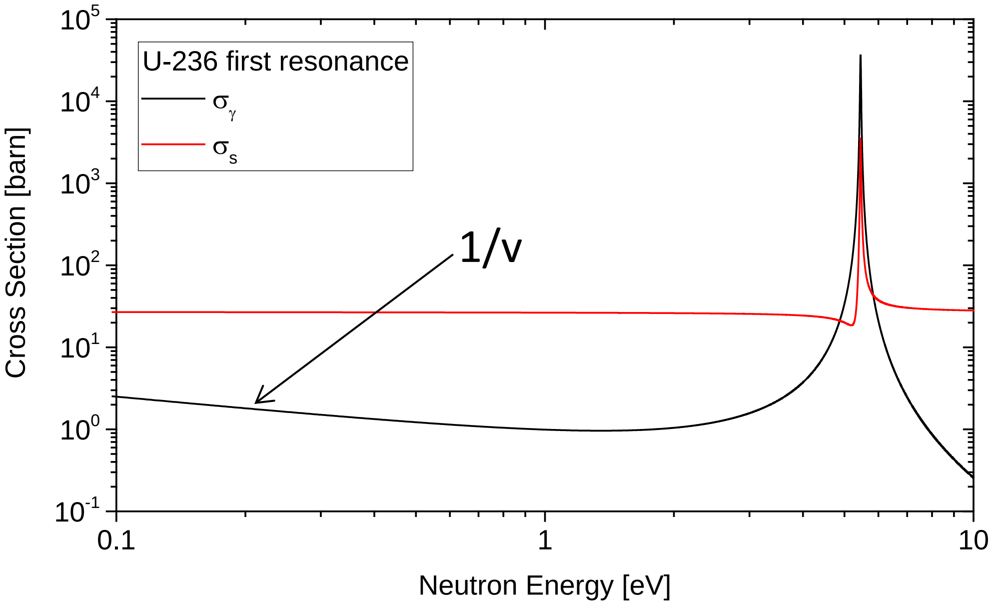

Cadmium Sample Information

- Sample purity: 0.9999 from Kamis Incorporated
- Natural metal samples:

  1.25% ^{106}Cd, 0.89% ^{108}Cd, 12.49% ^{110}Cd, 12.80% ^{111}Cd, 24.13% ^{112}Cd, 12.22% ^{113}Cd, 28.73% ^{114}Cd, 7.49% ^{116}Cd

- Sample thicknesses:

Nominal thickness (mm)	Areal density (atoms/barn)	Measurements
0.0254 (0.001 in.)	1.133E-4 ± 1E-7	Thermal capture
0.0508 (0.002 in.)	2.329E-4 ± 2E-7	Thermal transmission and capture
0.1016 (0.004 in.)	4.280E-4 ± 4E-7	Thermal transmission and capture, and epithermal capture
0.254 (0.010 in.)	1.1796E-3 ± 1.2E-6	Thermal transmission and epithermal capture
0.508 (0.020 in.)	2.3929E-3 ± 2.4E-6	Thermal and epithermal transmission, Thermal and epithermal capture
1.27 (0.050 in.)	5.8529E-3 ± 5.9E-6	Epithermal capture
2.54 (0.100 in.)	1.191E-2 ± 1E-5	Epithermal transmission
5.08 (0.200 in.)	2.4295E-2 ± 2.5E-5	Epithermal transmission and capture
10.16 (0.400 in.)	4.4260E-2 ± 4.5E-5	Epithermal transmission

Preparation of EXFOR Data and Headers

- Transmission and capture thermal and epithermal data files to be provided to the U.S. repository at Brookhaven National Laboratory

- Headers are to be sufficient to recreate the resonance parameter and uncertainty analysis

Traditional EXFOR Header

```
TITLE      Resonance parameters and uncertainties derived from
            epithermal neutron capture and transmission
            measurements of natural molybdenum
AUTHOR     (G.Leinweber, D.P.Barry, J.A.Burke, N.J.Drindak,
            Y.Danon, R.C.Block, N.C.Francis, B.E.Moretti)
INSTITUTE  (1USAKAP,1USARPI)
           (1USAUSA) US Military Academy, West Point, New York
REFERENCE  (J,NSE,164,287,2010)  Main reference
           (C,2007NICE,1,507,2007) Preliminary data
FACILITY   (LINAC,1USARPI) Rensselaer Polytechnic Institute LINAC
            facility
ANALYSIS   R-matrix Bayesian code SAMMY was used to extract
            resonance parameters from experimental spectra
HISTORY    (20100209C) Compiled by S.H.

REACTION   (42-MO-0(N,G),,RYL,,RAW)
SAMPLE      Natural Mo sample
            Physical type:        Metal
            Chemical composition: Element (Molybdenum)
            Thickness:          0.051 mm, (3.088E-04+-1E-07) at/b
            Sample mounted in aluminum sample cans. The thickness
            of aluminum on each of the front and rear faces of
            each sample was 0.38 mm.
INC-SOURCE (PHOTO) LINAC repetition rate:           200 pulses/sec
METHOD     (TRN,TOF) Flight path 25.567 m
DETECTOR   (NAICR) A 16-fold segmented NaI(Tl) multiplicity-
           type detector was used for capture measurements at
           25 m station
ERR-ANALYS (ERR-S) 1 sigma statistical errors (absolute errors)
STATUS     (TABLE) Not given in J,NSE,164,287,2010
                   Data obtained from D.P.Barry by e-mail
HISTORY    (20130111A) On. REACTION: ,TRN/RYL,,RAW -> ,RYL,,RAW
ENDBIB              17
COMMON               2          3
THICKNESS  TEMP
ATOMS/B    K
  3.088E-04  293.0
ENDCOMMON            3
DATA                 3       5436
EN         DATA       ERR-S
EV         NO-DIM     NO-DIM
 2.0127E+03 1.5993E-04 4.8325E-04
```

Standardized EXFOR Reporting

- A meeting of several experimentalists was held at IAEA in Vienna in October 2013 to discuss EXFOR reporting for resonance region experimental data (mostly transmission and capture).
  - Experimentalists: Guber (ORNL) ,Gunsing (CEA/nTOF), Kimura (JPARC), Noguere (CEA), Schillebeeckx (IRMM), Danon (RPI)
- The result of the meeting was a new template that capture the essential parameters of the different experiments
- Eu (Leinweber et al.) was the first RPI dataset to be reported using the new, more detailed measurement description
- ^{95}Mo (Bahran et al.) was the second.

A. EXPERIMENT DESCRIPTION

1. Main Reference		1
2. Facility	RPI	1,2,3
3. Neutron production		
Neutron production beam	Electron	
Nominal beam energy	56 MeV	
Repetition rate (pulse/sec)	25	
Pulse width	560 ns	
Nominal beam power	470 W	
Primary neutron production target	tantalum	
Neutron source position in moderator	Enhanced thermal target	4,5
4. Moderator		
Material	graphite	
Dimension (thickness, height×width×depth,…)	Integral, see refs 4,5	
Mass		
Temperature (K)	20° Celsius	
Target nominal neutron production intensity (n/sec)	10^{13}	
Moderator-room decoupler (Cd, B, …)		
5. Other experimental details		
Measurement type	Capture	
Method (total energy, total absorption, …)		
Effective flight path length (m)	14.96 ± 0.02 m	
Flight path angle with respect to moderator surface	Neutron beam is perpendicular to the moderator surface.	
Neutron beam dimensions at sample position (mm × mm, diameter in mm, …)	Diameter of 2.54 mm	

SAMMY Gaussian + tail

- SAMMY has a form for Gaussian and exponential

$$f_{GE}(E) = \frac{1}{\Delta_E \Delta_G \pi} \int_{E-\Delta E_S}^{\infty} dE'' \exp\left\{ -\frac{(E'' - (E - \Delta E_S))}{\Delta_E} \right\}$$
$$\times \int_{-\infty}^{+\infty} dE' \exp\left\{ -\frac{(E' - E'')^2}{\Delta_G^2} \right\} f(E')$$

- Δ_G – Gaussian width (moderator (ΔL) + channel width (Δt_c) + burst width (Δt_G) + other E dist (Δ_c))

$$\Delta_{all}^2 = \frac{2}{3} E^2 \left(\frac{\Delta L}{L} \right)^2 + \frac{2}{m} E^3 \frac{2}{3} \left(\frac{\Delta t_c}{L} \right)^2 + \frac{2}{m} E^3 \frac{1}{\ln 2} \left(\frac{\Delta t_G}{L} \right)^2 + \Delta_C^2 \quad ,$$

- Δ_E – exponential width (moderator + detector)

$$\Delta t_E = D_1 E + D_0 + D_2 \ln(E) \qquad \Delta_E = \frac{2E^{3/2}}{L(m/2)^{1/2}} \Delta t_E$$

- ΔE_S – shift center (use shift)

Example: SAMMY Gaussian + Exponential Resolution Parameters

	Thermal Capture	Epi-Thermal Capture	Epi-Thermal Transmission
DELTAL Flight path length	0.0055	0.0055	0.0055
DELTAG burst width	0.0254	0.0254	0.0254
DELTAE Exponential	0.1	0.1	0.1
DELTE:**DELE0**	0.06	0.06	0.18650
DELTE:**DELE1**	0	0	1.2687e-6
DELTE:**DELE2**	0	0	0.02069

EXPONENTIAL FOLDING width is energy dependent
DO NOT SHIFT ENERGY for exponential tail

Example: RPI Resolution Function
Thermal Region Transmission

- Complicated function with many parameters (Enhanced thermal target + detector)

$$I_2(t) = A_0 \left\{ \frac{(t+\tau)^2}{2!\Lambda^3} e^{-(t+\tau)/\Lambda} + A_1 \left[A_2 e^{-A_3(t+t_0)} + A_4 e^{-A_5(t+t_0)} \right] X(t) + \sum_{i=1}^{5} B_{2i-1} e^{-B_{2i}(t+t_0)} \right\},$$

$$\Lambda(E) = \Lambda_0 + \Lambda_1 \ln(E) + \Lambda_2 [\ln(E)]^2 + \Lambda_3 E^{\Lambda_4} \qquad \tau(E) = \tau_1 e^{-\tau_2 E} + \tau_3 e^{-\tau_4 E} + \tau_5 + \tau_6 E^{\tau_7} \qquad A_i(E) = \left\{ a_{i1} e^{-a_{i2} E} + a_{i2} e^{-a_{i4} E} + a_{i5} + a_{i6} E^{a_{i7}} \right\} \alpha_i$$

Param	Value	Param	Value	Param	Value	Param	Value
τ_1	320.94	Λ_0	679.98	a_1	-000078	A_0	935.91
τ_2	0.02426	Λ_1	-226.21	a_2	0.02407	A_1	-69.068
τ_3	318.46	Λ_2	21.09	a_3	-0.00063	A_2	0.005
τ_4	0.02922			a_4	3.53	A_3	0.39485
τ_5	235.71			a_5	0.000112	A_4	0.0075

Bayesian vs Frequentist Data Analysis

- Should measurement reports be independent assessments of resonance parameters or mini-evaluations ?
  - Independent assessment needed to isolate the contribution of the current measurement
  - Bayesian theory insists that prior knowledge be included
  - Publication bias